

Surface-Plasmon-Mediated Single-Molecule Fluorescence Through a Thin Metallic Film

F.D. Stefani, K. Vasilev, N. Bocchio, N. Stoyanova, and M. Kreiter*

Max Planck Institute for Polymer Research, Ackermannweg 10, D-55128 Mainz, Germany

(Received 7 July 2004; published 19 January 2005)

We demonstrate that fluorescence of single molecules in the nanometric vicinity of a thin gold film can be effectively excited and detected through the film with an epi-illumination scanning confocal microscope. A full theoretical treatment of the fluorescence signal indicates that both excitation and emission are surface-plasmon mediated. Remarkably, the number of photons detectable from chromophores perpendicular to the interface is enhanced by the presence of the metal.

DOI: 10.1103/PhysRevLett.94.023005

PACS numbers: 32.50.+d, 73.20.Mf, 87.64.Tt

A metallic object near a fluorescent dye can influence both its excitation and emission, eventually leading to a significantly enhanced performance with the consequent technological impact, e.g., in solar cells and light emitting devices. Thus, a thorough investigation of the underlying physics is of great importance. Maximum information is obtained via experiments on a single-molecule level because they yield information otherwise hidden in the ensemble [1]. By using metallic tips, the fluorescence intensity [2] and excited state lifetime [3] of single dyes was manipulated on a subwavelength scale. However, a rigorous mathematical treatment of chromophores near nontrivial metal objects such as scanning probe tips is highly demanding or even impossible if the true local geometry is not known. Planar systems, on the other hand, have been studied for several decades because it is possible to prepare them with high precision and reproducibility. They proved to be a nearly perfect platform for the quantitative study of photophysical effects such as excitation enhancement, energy redistribution, and quenching [4–7]. Surprisingly, only one work addressing single-molecule fluorescence near a metal surface was reported [8] which showed significant deviations from a later theoretical treatment [9].

In this Letter, we explore experimentally and theoretically the excitation and emission of single-molecule fluorescence through a thin metallic film with an epiconfocal configuration [Fig. 1(a)]. The finding that due to surface-plasmon enhancement the fluorescence signals of individual chromophores are detectable with a good signal-to-noise ratio and may even be enhanced compared to the situation without gold is of potential impact for the design of solid state devices, bio or chemical sensors, and single-molecule detection schemes in general. In contrast to [8], continuous illumination of a large area of the sample is avoided with the consequent reduction of unnecessary irreversible photo-bleaching. Furthermore, the chromophores' side of the sample remains accessible to complementary techniques such as scanning probe microscopies. Since the chromophores are placed in a well defined layered system, a quantitative theoretical treatment is possible

that opens the door to the design of single-molecule fluorescence experiments near metallic surfaces.

The samples consist of chromophores separated from a 44-nm-thick gold film by a 24-nm-thick polyelectrolyte spacer layer, all on a glass substrate [Fig. 1(a)]. The preparation follows a published method [10] with two slight modifications in order to reduce the fluorescence background to be suited for single-molecule experiments. First, the gold film was thermally evaporated on the glass substrates. Second, the polyelectrolytes were purified before use. Poly(allylamine) (PAH, Aldrich, MW 70 000) was dialyzed with a membrane tube with a cutoff molecular weight of 3500 (Spectrum Lab. Inc., Spectra/por6). Poly(styrenesulfonate) (PSS, Aldrich, MW 70 000), was dissolved in water and transferred dropwise into cool (218 ± 5 K) ethanol. The precipitated polymer was then filtered and dried in vacuum. Fluorescent 1, 1, 3, 3, 3-hexamethylindocarbocyanine iodide (DiIC1(5), Molecular Probes) molecules were deposited electrostatically on the negatively charged, PSS-terminated surface of the multilayer by immersing the samples in a

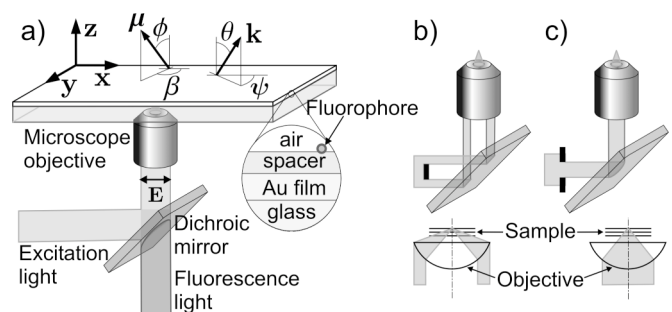


FIG. 1. (a) Experimental geometry and coordinate system. The x axis is parallel to the polarization direction of the electric field \mathbf{E} of the excitation beam and the z axis is perpendicular to the interfaces. The orientation of the transition dipole of the chromophores $\boldsymbol{\mu}$ and the wave vector of the incident or emitted radiation \mathbf{k} are defined by the pairs of angles (β, ϕ) and (ψ, θ) , respectively. Here, full-beam (FB) illumination is sketched. (b) High-angle of incidence illumination [plasmon light (PL)]. (c) Low angle of incidence illumination [no plasmon light (NPL)].

10^{-10} M, Milli-Q water solution of the dye for 1 min. The properties of the layers as determined in earlier studies [10] are listed in Table I.

The experiments were conducted on a home-built sample scanning confocal microscope. Linearly polarized, $\lambda = 633$ nm light from a He-Ne laser (Uniphase Inc.) is focused through the glass substrate and impinges on the gold film in order to excite the molecules on the other side of the gold film. Single-molecule fluorescence images were obtained with three different illumination modes corresponding to different incidence angle ranges. Full illumination of the rear lens of the microscope objective (Nikon Plan-Apo 100×1.4 NA) [full-beam illumination (FB), Fig. 1(a)] produces angles of incidence $0^\circ < \theta < 68.8^\circ$. On this sample, surface plasmons are excited by plane waves incident on the sample with $45^\circ < \theta < 55^\circ$ [10], leading to an enhancement of the incident field up to a factor of 9 at the Au-spacer interface. For all other θ , the Au film acts as good mirror and little light is transmitted. In order to elucidate the role of surface-plasmon excitation, a blocking disk and a reduced illumination beam were used to produce incidence angles $31.6^\circ < \theta < 68.8^\circ$ [plasmon light (PL), Fig. 1(b)] and $0^\circ < \theta < 31.6^\circ$ [no plasmon light (NPL), Fig. 1(c)], respectively. Figure 2 shows a typical FB image of the samples. The great majority of the observed patterns have the same shape but different intensities. From the symmetry of the patterns [11] it can be deduced that they are due to the z component of the electrical field while the x and y components are strongly suppressed. The large size of the patterns indicates that only a limited range of exciting plane waves contributes significantly to the excitation, pointing toward surface-plasmon mediated excitation.

In order to fully model these observations, the excitation patterns have to be calculated as in [11], where similar patterns were calculated for high-angle illumination of a dielectric interface and directly compared to experimental results. In our case, the deexcitation rates, which are strongly influenced by the gold, must be included as an additional factor in a theoretical model that is outlined in the following. In the absence of triplet blinking, the detectable fluorescence intensity I_{SM} emitted by a single molecule is

$$I_{SM} = \Gamma_{ex} \eta P_{obj}, \quad (1)$$

where Γ_{ex} is the excitation rate, P_{obj} is the probability that

TABLE I. Thickness (d) and dielectric constants (ϵ) of the sample layers for the excitation and emission wavelengths.

Layer	d [nm]	$\epsilon(\lambda_{ex} = 633 \text{ nm})$	$\epsilon(\lambda_{em} = 670 \text{ nm})$
Glass	∞	2.26	2.25
Gold	44	$-12.65 + i 1.01$	$-14.94 + i 1.1$
Spacer	24	2.38	2.32
Air	∞	1	1

the molecular excitation leads to emission of a photon into the collection solid angle of the objective, and η is the detection probability. In order to model the single-molecule fluorescence signal, Γ_{ex} and P_{obj} are calculated by considering the chromophores (both in their ground and excited state) as oscillating dipoles with moment $\boldsymbol{\mu}$ interacting classically with the electromagnetic field. Then Γ_{ex} is given by:

$$\Gamma_{ex}(\mathbf{r}) \propto |\boldsymbol{\mu} \cdot \mathbf{E}(\mathbf{r})|^2. \quad (2)$$

The electric field $\mathbf{E}(\mathbf{r})$ at position \mathbf{r} from the Gaussian focal point of the microscope objective can be calculated by adding the contributions of an angular distribution of electromagnetic plane waves by [12]:

$$E_j(\mathbf{r}) = C \int_0^{2\pi} \int_{\theta_{min}}^{\theta_{max}} \sqrt{\cos\theta} E_j^0(\theta, \psi) e^{i\mathbf{k} \cdot \mathbf{r}} \sin\theta d\theta d\psi, \quad (3)$$

where j denotes the Cartesian component ($j \in \{x, y, z\}$) of \mathbf{E} , C is a constant, and \mathbf{k} is the wave vector. The propagation direction given by ψ and θ (see Fig. 1) is integrated according to the illumination mode. $E_j^0(\theta, \psi)$ are the Cartesian components of the plane waves at $\mathbf{r} = 0$ given by

$$\begin{aligned} E_x^0 &= E_{\parallel}^p(\theta) \cos^2\psi + E_{\parallel}^s(\theta) \sin^2\psi \\ E_y^0 &= [E_{\parallel}^p(\theta) - E_{\parallel}^s(\theta)] \cos\psi \sin\psi & E_z^0 &= E_{\perp}^p(\theta) \cos\psi, \end{aligned} \quad (4)$$

where E_{\parallel}^p , E_{\parallel}^s , and E_{\perp}^p are the p - and s -polarized components of the electric field parallel and perpendicular to the interfaces, respectively. They are calculated by solving Maxwell equations for the multilayer system via a transfer matrix algorithm [13] for a plane wave incident with θ and unitary p - and s -polarized amplitudes. For a given wavelength, E_j^0 are functions of θ , ψ , thickness, and dielectric constants of the layers.

Assuming a chromophore with unit quantum efficiency, the collection probability P_{obj} [Eq. (1)] is given by a balance of decay rates Γ :

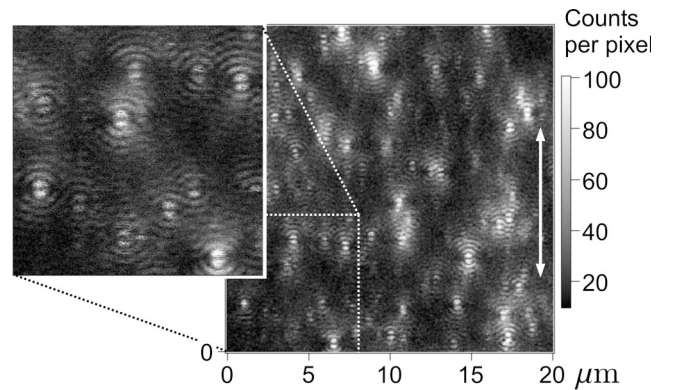


FIG. 2. Single-molecule fluorescence image obtained with FB illumination. The white arrow indicates the polarization direction of the excitation beam.

$$P_{\text{obj}} = \frac{\Gamma_{\text{obj}}}{\Gamma_{\text{tot}}} = \frac{\Gamma_{\text{obj}}}{\Gamma_{\text{glass}} + \Gamma_{\text{air}} + \Gamma_{\text{nr}}}. \quad (5)$$

The subscripts distinguish possible decay channels for the excited chromophore: total rate (tot), photon emission into the collection solid angle (obj) and to the glass-air semi-space (glass-air), and decay that does not lead to far field radiation (nr). The decay rates of a molecule with arbitrary out of plane orientation ϕ are calculated from the two limiting cases of dipoles parallel (Γ^{\parallel}) and perpendicular (Γ^{\perp}) to the interface [14]:

$$\Gamma(\phi) = \sin^2(\phi)\Gamma^{\parallel} + \cos^2(\phi)\Gamma^{\perp}. \quad (6)$$

By application of Lorentz reciprocity theorem, the radiative decay leading to far field photons in glass or in air in a given cone defined by θ is calculated by the evaluation of the equivalent problem of exciting the dipole with a plane wave from that direction. This leads to the following expressions for the rate of light emitted to a region of space defined by $(\theta_{\min}, \theta_{\max})$:

$$\Gamma_m^{\parallel} = \frac{3n_m}{8} \int_{\theta_{\min}}^{\theta_{\max}} [|E_{\parallel}^p(\theta)|^2 + |E_{\parallel}^s(\theta)|^2] \sin\theta d\theta$$

$$\Gamma_m^{\perp} = \frac{3n_m}{4} \int_{\theta_{\min}}^{\theta_{\max}} |E_{\perp}^p(\theta)|^2 \sin\theta d\theta, \quad (7)$$

where Γ_m^{\parallel} and Γ_m^{\perp} are normalized to the decay rate in vacuum so they do not depend on μ . n_m is the refractive index of medium m (air or glass). E_{\parallel}^p , E_{\parallel}^s , and E_{\perp}^p are now calculated for the emission wavelength and plane waves incident on the multilayer from medium m . Introducing the appropriate m , θ_{\min} , and θ_{\max} , these integrals are used to obtain Γ_{air} , Γ_{glass} , and Γ_{obj} . The normalized total decay rate Γ_{tot} is calculated following the back-reacted field approach [14] as described in [10]. Figure 3 shows all the relevant decay rates as a function of the spacer thickness, calculated using the experimentally determined parameters [10] given in Table I. At separation distances below 10 nm, nonradiative energy transfer to the gold dominates. For larger separation distances the radiative fraction of the decay increases and at the experimental separation of 24 nm,

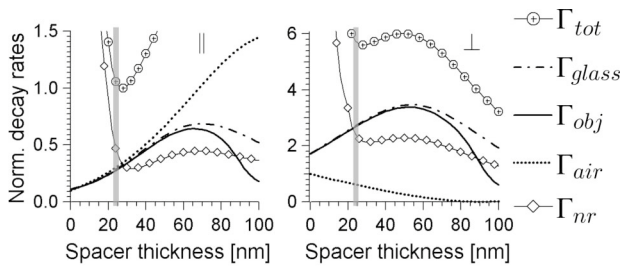


FIG. 3. Deexcitation rates of a parallel (left) and perpendicular (right) dipole as a function of the spacer thickness. The vertical bands show the spacer thickness used in the experiments.

P_{obj} equals 0.26 for a parallel dipole and 0.47 for a perpendicular one.

The modeled single-molecule fluorescence signal is then calculated by means of Eq. (1). Since η is unknown, the calculated signals describe the experiments up to a constant proportionality factor. In Fig. 4, calculated fluorescence signals are shown for a representative selection of molecular orientations (left) together with experimental images of the same region of a sample obtained with the three illumination modes (right). The experimental FB and PL images are very similar, both showing a strong signal with the characteristic pattern discussed above (Fig. 2). The PL background is lower ($\sim 1/2$), due to the considerably smaller amount of reflected light. The NPL image shows round signals with a much weaker intensity; the most intense of those coincide with very weak features in the FB and PL image while only a very weak signal is seen at the position corresponding to the bright FB and PL pattern. By comparison to the calculated signals for different orientations of μ , the observed signals can be assigned to molecules with different orientations. With surface-plasmon mediated excitation (PL and FB), molecules ori-

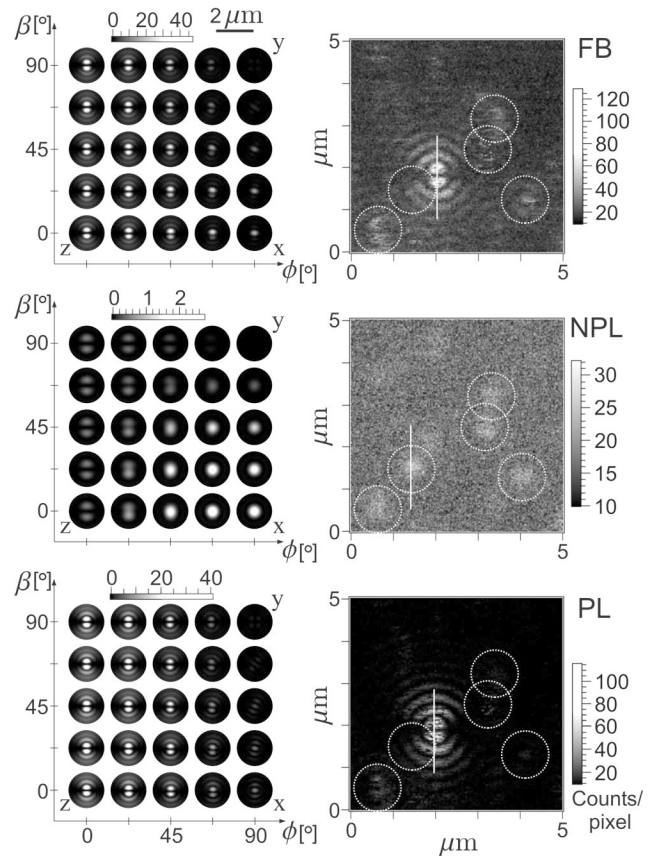


FIG. 4. Modeled single-molecule fluorescence signals for different dipole orientations (left) and experimental images (right) for the three illumination modes. More details are given in the text.

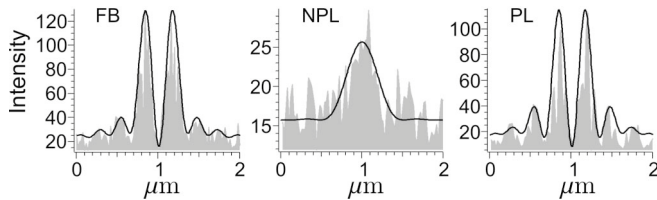


FIG. 5. Comparison of the experimental and modeled single-molecule fluorescence signals for the three illumination modes. The modeled signals were scaled with one common scaling factor. A background intensity as determined independently for each experimental image (FB: 16, NPL: 15.2, PL: 7.7) was added.

ented close to the z axis lead to very strong extended patterns; this effect is due to the dominant z component of the surface-plasmon at $\lambda = 633$ nm. The weak round patterns found experimentally for NPL illumination are in agreement with the theory as well and can be assigned to the molecules oriented close to the x axis. Experimental profiles corresponding to typical z and x patterns are extracted along the lines indicated in Fig. 4 and compared to the theoretical prediction in Fig. 5. The modeled profiles were scaled with a common factor and the experimentally determined background was added. The good agreement shows the applicability of the theoretical model to the experiment.

A possible measure for the efficiency of single-molecule fluorescence detection is the number of detectable photons emitted by a molecule; therefore, the number of excitation-deexcitation cycles the molecule can perform before undergoing irreversible photo-bleaching has to be considered. Since it is found for this dye that photo-bleaching occurs at a constant rate from the excited state [15], an enhancement of the total deexcitation rate is accompanied by an increase in the number of cycles (nc):

$$nc \propto \Gamma_{\text{tot}} \quad (8)$$

and for a given I_{SM} , the number of detectable photons n_{hv} emitted by a single molecule is

$$n_{hv} = nc \frac{\Gamma_{\text{obj}}}{\Gamma_{\text{tot}}}(\phi) \propto \Gamma_{\text{obj}}(\phi). \quad (9)$$

Calculations of Γ_{obj} for samples with and without the gold film show that the number of detectable photons emitted by a parallel molecule in the sample with the gold film is 26% of the photons the same molecule would emit in the sample without the gold film. For the case of a perpendicular molecule, due to the surface-plasmon enhancement, this percentage rises to 140%, thus exceeding the value obtained without gold.

For the same sample geometry, detection from the air side was compared to the detection through the gold film.

The fraction of the decay rate of a fluorophore corresponding to fluorescence collected by a 0.9 NA objective from the air side was calculated by Eqs. (6) and (7) ($\theta_{\text{min}} = 0^\circ$, $\theta_{\text{max}} = 64.2^\circ$). The surface-plasmon mediated detection through the gold film is more effective for all dipole orientations and more than six times more effective for the perpendicular case.

We can conclude that due to the role of surface plasmons in the excitation and emission processes, efficient single-molecule fluorescence experiments through a thin gold film are possible. It was found that the metal enhances the number of detectable photons for dyes oriented perpendicular to the interface. This experimental geometry should be particularly useful for experiments in which single molecules are used as markers to follow dynamical processes near a metallic surface because no optical parts are required on the side where complementary techniques are applied. Quantitative studies on molecular photodynamics near metals are envisaged which should contribute to a more quantitative understanding of the more pronounced effects in the vicinity of complex metal objects.

This work was financially supported by the Bundesministerium für Bildung und Forschung (Grant No. 03N8702).

*E-mail: kreiter@mpip-mainz.mpg.de

- [1] X. S. Xie and J. K. Trautman, *Annu. Rev. Phys. Chem.* **49**, 441 (1998).
- [2] A. Kramer, W. Trabesinger, B. Hecht, and U.P. Wild, *Appl. Phys. Lett.* **80**, 1652 (2002).
- [3] W. Trabesinger, A. Kramer, M. Kreiter, B. Hecht, and U.P. Wild, *Appl. Phys. Lett.* **81**, 2118 (2002).
- [4] K. Drexhage, H. Kuhn, and F. Schäfer, *Ber. Bunsenges. Phys. Chem.* **72**, 329 (1968).
- [5] R.R. Chance, A. Prock, and R. Silbey, *Adv. Chem. Phys.* **37**, 1 (1978).
- [6] W. Knoll, *Annu. Rev. Phys. Chem.* **49**, 569 (1998).
- [7] W.L. Barnes, *J. Mod. Opt.* **45**, 661 (1998).
- [8] H. Yokota, K. Saito, and T. Yanagida, *Phys. Rev. Lett.* **80**, 4606 (1998).
- [9] J. Enderlein, *Biophys. J.* **78**, 2151 (2000).
- [10] K. Vasilev, W. Knoll, and M. Kreiter, *J. Chem. Phys.* **120**, 3439 (2004).
- [11] B. Sick, B. Hecht, and L. Novotny, *Phys. Rev. Lett.* **85**, 4482 (2000).
- [12] E. Wolf, *Proc. R. Soc. London A* **253**, 349 (1959).
- [13] P. Yeh, *Optical Waves in Layered Media* (John Wiley and Sons, New York, 1988).
- [14] L. Novotny, Ph.D. thesis, Swiss Federal Institute of Technology, Zurich, 1996.
- [15] K. Vasilev, F.D. Stefani, V. Jacobsen, W. Knoll, and M. Kreiter, *J. Chem. Phys.* **120**, 6701 (2004).